

Squeezing oscillations in a multimode bosonic Josephson junction

Tiantian Zhang,* Mira Maiwöger, Filippo Borselli, Yevhenii Kuriatnikov, Jörg Schmiedmayer, and Maximilian Prüfer
*Vienna Center for Quantum Science and Technology,
Technische Universität Wien, Atominstitut, Vienna, Austria.*

(Dated: April 7, 2023)

Quantum simulators built from ultracold atoms promise to study quantum phenomena in interacting many-body systems. However, it remains a challenge to experimentally prepare strongly correlated continuous systems such that the properties are dominated by quantum fluctuations. Here, we show how to enhance the quantum correlations in a multimode bosonic Josephson junction; our approach is based on the ability to track the dynamics of quantum properties. After creating a bosonic Josephson junction at the stable fixed point of the classical phase space, we observe squeezing oscillations in the two conjugate variables. We show that the squeezing oscillation frequency can be tuned by more than one order of magnitude and we are able to achieve a spin squeezing close to 10 dB by utilizing this oscillatory dynamics. The impact of improved spin squeezing is directly revealed by detecting enhanced spatial phase correlations between decoupled condensates. Our work provides new ways for engineering correlations and entanglement in the external degree-of-freedom of interacting many-body systems.

Understanding the role of quantum fluctuations and entanglement in interacting many-body systems is of critical importance for the development of quantum technologies, such as quantum metrology [1, 2] and quantum simulation [3]. Especially the ability to prepare entanglement[4] in quantum many-body systems is pivotal. In this context, ultracold atoms have proven to be a versatile platform[1], where for instance experimental studies on the internal spin degree of freedom(DoF) [5–8] have led to great insights. Creating entangled quantum states in the external DoF [9] is on the contrary less explored; one interesting platform is tunnel-coupled BECs in double wells (DWs). Especially in the one-dimensional (1D) regime, tunnel-coupled BECs are excellent quantum simulators [10, 11] for the sine-Gordon field theory [12, 13].

In this work, we study quantum dynamics in split 1D BECs in DWs, realising a multimode bosonic Josephson junction (BJJ) [14, 15]. Instead of studying classical Josephson oscillations [16–21], we prepare the system at the stable fixed point of the classical phase space and access its quantum properties. Despite the stationary expectation values of both relevant observables, relative number and relative phase, we observe oscillatory dynamics of the quantum fluctuations. We present an improved splitting routine that capitalizes this dynamics in the BJJ to foster strong spin squeezing in decoupled condensates, where the quantum properties are otherwise dominated by thermal noise. Finally, the spatially resolved detection of the relative phase enables us to demonstrate how this improved spin squeezing enhances spatial correlations between two decoupled 1D condensates.

REALISATION AND READOUT OF AN ELONGATED BJJ

We realise a multimode BJJ with 1D BECs of typically $2000 - 5000$ ^{87}Rb atoms trapped magnetically under an Atom Chip [22]. The DW potential is generated by employing Radio-Frequency (RF) dressing[23] on a static magnetic trap with trap frequencies $[f_\perp, f_z] = [4.14 \cdot 10^3, 15]$ Hz. Precise transformation from a single well to a DW is achieved by ramping up the amplitude \mathcal{A} of the RF field whose value is normalised to the maximal current. We display in Fig. 1a the transverse trap configuration and typical experimental readout with our single-atom-sensitive fluorescence imaging system [24] after Time-of-Flight (ToF) of $t_F = 43.4$ ms. Two separate experimental routines are employed to read out either of the two conjugate observables [25]: the relative atom number, $N_- = N_L - N_R$, or the relative phase, $\Phi = \Phi_L - \Phi_R$, between the left (L) and right (R) condensate in the DW. (see Methods for details).

The macroscopic dynamics in BJJ can be described by the two-mode Bose-Hubbard (BH) model

$$\mathcal{H} = \frac{2J}{\hbar} \left[\frac{UN}{4J} n^2 - \sqrt{1 - n^2} \cos \Phi \right], \quad (1)$$

where $n = N_-/N$ is the relative imbalance, U is the interaction strength and J is the single particle tunnel coupling strength. From Eq.(1), we can obtain the Josephson oscillation frequency of the mean field values $\langle \Phi \rangle$ and $\langle N_- \rangle$ [14, 15]

$$f_p = \frac{2J}{\hbar} \sqrt{\cos \Phi_0 + UN/2J}, \quad (2)$$

known as the plasma frequency. Here $\cos \Phi_0$ indicates the initial phase coherence factor. From Eq.(2), we see that f_p depends explicitly on the single particle tunnel coupling strength J and the total atom number N .

* tiantian.zhang@tuwien.ac.at

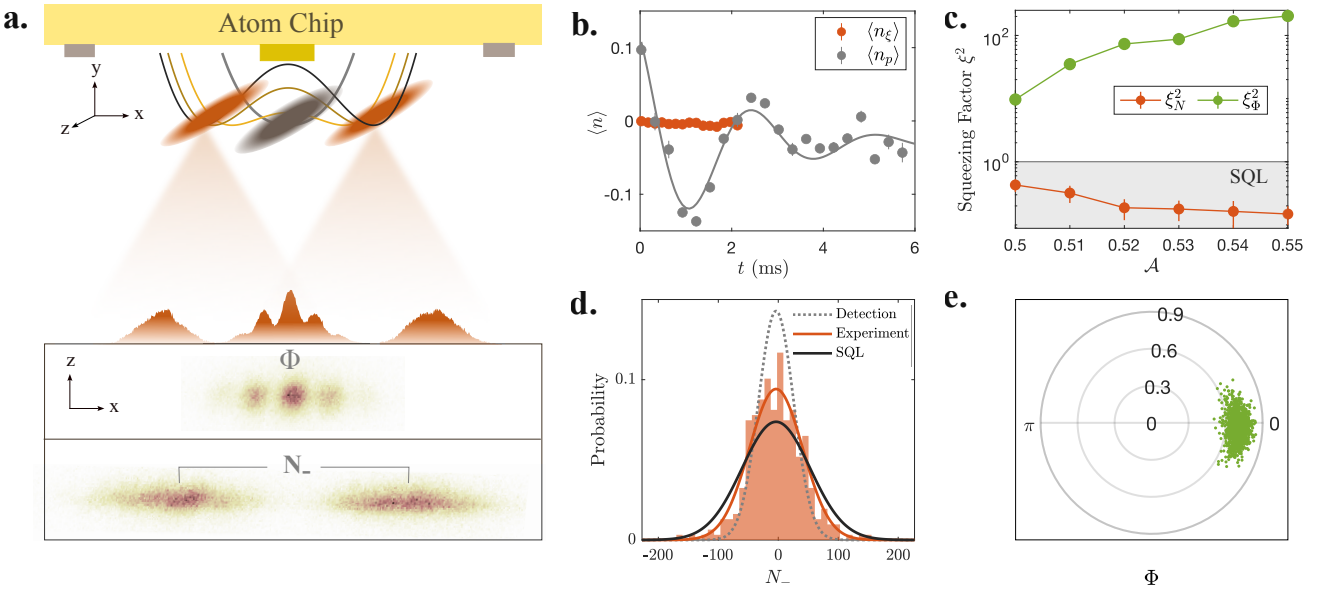


FIG. 1. Preparation and readout of spin-squeezed state. **a.** A single 1D BEC trapped below an Atom Chip is split by raising the amplitude of the RF field to transform a single well to a DW. Experimental readout of the relative phase, Φ and relative atom number N_- , with fluorescence imaging after long ToF. **b.** Evolution of expectation value of relative imbalance $\langle n \rangle = \langle N_- / N \rangle$ in coupled DW. Grey markers, $\langle n_p \rangle$, show Josephson oscillation with an imprinted nonzero initial imbalance and orange markers, $\langle n_\xi \rangle$, indicate that the expectation values are at equilibrium after symmetrical splitting. **c.** Measured squeezing factors of N_- and Φ , denoted as ξ_N^2 and ξ_Φ^2 , in various DWs after splitting with speed $\kappa = 0.02 \text{ ms}^{-1}$. The measurement is consistent with the expectation that repulsively interacting BECs in DWs are number squeezed, $\xi_N^2 < 1$. Grey solid line indicates the standard quantum limit. **d.** Histogram of N_- together with fitted normal distribution (orange). As a reference we show a binomial distribution (black; indicating the SQL) and a normal distribution with the width corresponding to the detection noise level (grey). **e.** Polar distribution of Φ with fringe visibility C as radii (see Methods). Errorbars represent one standard error of mean (s.e.m.).

PREPARING QUANTUM-CORRELATED STATES

To prepare strongly correlated BECs, we split up a single BEC into two by transforming a single well into a DW (see Fig. 1a). The relative DoF of the two split BECs is then dominated by quantum fluctuations. This is in contrast to preparing BECs in DWs via direct cooling, which is suitable for studying systems at thermal equilibrium [11], but introduces thermal fluctuations on N_- [26].

We emphasize that symmetric splitting is performed here, so $\langle N_- \rangle = \langle \Phi \rangle = 0$ as opposed to previous work on Josephson oscillations in elongated BJJ [21]. We show in Fig. 1 b an example of Josephson oscillation of relative imbalance $\langle n_p \rangle$ by imprinting an initial nonzero imbalance, which is used for extraction of the plasma frequency f_p . For comparison, we also display the typical evolution of the imbalance, $\langle n_\xi \rangle \approx 0$, in the case of symmetric splitting investigated in this work.

To quantify the fluctuations of the observables, we define the squeezing factors

$$\xi_N^2 = \frac{\Delta^2 N_-}{N}, \quad \xi_\Phi^2 = \Delta^2 \Phi \cdot N, \quad (3)$$

where $N = N_L + N_R$ is the total atom number and

$\Delta^2 N_-$ and $\Delta^2 \Phi$ represent the statistical variance. If the two condensates are uncorrelated, the projection noise of N_- and Φ follows a Binomial distribution with respective variance N and $1/N$. Therefore $\xi_N^2 = \xi_\Phi^2 = 1$ represents the standard quantum limit (SQL). Spin-squeezed states are characterised [27, 28] as $\xi_s^2 = \xi_N^2 / \langle \cos \Phi \rangle^2 < 1$, where $\langle \cos \Phi \rangle$ is the phase coherence factor.

In the case of adiabatic splitting, the system follows the ground state of the many-body Hamiltonian[29] and becomes more strongly number squeezed in less coupled DWs owing to repulsive interatomic interactions. In Fig. 1c, we show the experimentally inferred variance of N_- and Φ in various DWs with ramp speed $\kappa = \delta \mathcal{A} / \delta t = 0.02 \text{ ms}^{-1}$. To ensure reliable statistics, we conduct ~ 200 repetitions for each measurement. The experimentally measured fluctuations of split BECs agree with the trend of theoretical prediction and yield better number squeezing, i.e. smaller ξ_N^2 , and broadened phase distribution, i.e. larger ξ_Φ^2 , in less coupled DWs.

During the ram-up of the RF amplitude \mathcal{A} , the two lowest single particle eigenstates of the DW potential become energetically degenerate. This means that adiabaticity will be broken except for infinitely slow ramps. In opposition, in order to prevent phase diffusion induced by interatomic interactions, a fast ramp is desirable. Considering these two competing effects during the sim-

gle linear ramp-up, we seek after alternative approaches to optimally prepare spin-squeezed states of BECs in decoupled DWs. In the next section, we demonstrate an improved approach based on the emerging dynamics of quantum fluctuations in tunnel-coupled DWs. A similar approach has been used in single-mode spin BECs to prepare spin-squeezed ground states [30, 31].

SQUEEZING OSCILLATIONS IN CONJUGATE QUADRATURES

We prepare two BECs in a strongly coupled DW ($\mathcal{A} = 0.5$) by linearly ramping up from a single well at speed $\kappa = 0.02 \text{ ms}^{-1}$; this prepares the system at the stable fixed point of the classical phase space, i. e. $\langle N_- \rangle = 0$ and $\langle \Phi \rangle = 0$. Since the splitting process is non-adiabatic, it results in phase space fluctuations different from the ground state. We show in Fig. 2a that this leads to dynamics of the quantum fluctuations of the conjugate observables. The squeezing factors in both quadratures undergo oscillatory dynamics which we attribute to the Josephson dynamics. We can understand this dynamics

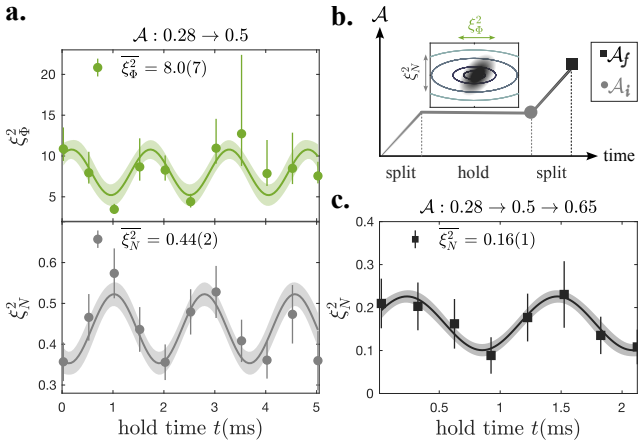


FIG. 2. Squeezing oscillations and two-step sequence. **a.** Measured number (gray circle) and phase (green circle) squeezing factors as a function of hold time in strongly coupled DW ($\mathcal{A} = 0.5$) after a linear ramp from a single well with speed $\kappa = 0.02 \text{ ms}^{-1}$. Average squeezing values are indicated as $\overline{\xi^2}$. We observe squeezing oscillations in both quadratures with comparable frequencies and a phase shift of π . **b.** Schematic of the two-step splitting procedure. The inset shows quantum state distribution in the classical phase space from BH model (Eq. 1). **c.** Measured number squeezing oscillations, stemming from the hold time in the coupled DW, after two-step splitting with ramp speed $\kappa = 0.02 \text{ ms}^{-1}$ to $\mathcal{A}_f = 0.65$. All solid lines are fits with a sine function and bands indicate 68% prediction confidence interval. Errorbars represent one s. e. m.

with the intuitive picture that a π rotation of a single realisation corresponds to a 2π rotation of quantum state distribution in phase space (inset in Fig. 2c), and thereby deduce that the squeezing oscillations are twice as fast

as the Josephson oscillations of the mean (see Ext. Data Fig. 2).

We fit the observed squeezing factors in Fig. 2a with a sine function to determine the squeezing oscillation frequency and obtain $f_\xi = 567(29) \text{ Hz}$ in relative number N_- quadrature with total atom number $N = 4154(35)$ and $f_\xi = 649(33) \text{ Hz}$ in relative phase Φ quadrature with $N = 4302(45)$ (see Methods). The measured squeezing oscillations in both quadratures are as expected on the order of twice the experimentally measured plasma frequency f_p and have a π phase shift with respect to each other. Combining the complementary measurement in Fig. 2a, we infer that quantum state fluctuations stay just above the Heisenberg limit $\overline{\xi_N^2} \cdot \overline{\xi_\Phi^2} \approx 3.5$ with $\overline{\xi_N^2} = 0.43(2)$ and $\overline{\xi_\Phi^2} = 8.0(7)$.

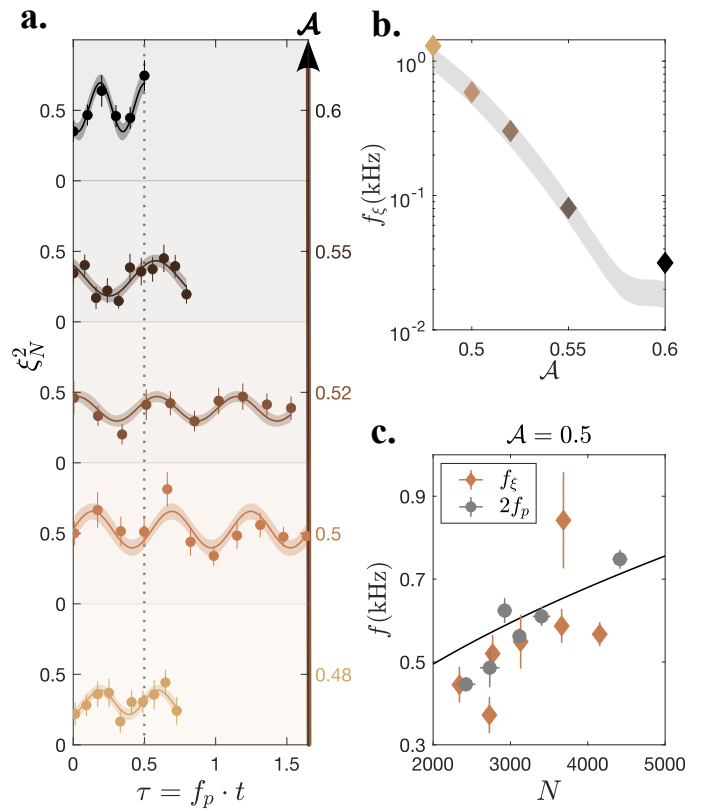


FIG. 3. Tuning squeezing oscillation frequency **a.** Observed number squeezing factor ξ_N^2 evolution in coupled DWs with increasing \mathcal{A} (bottom to top). The solid line is a fitted sine function with 68% simultaneous prediction bounds. **b.** The extracted squeezing frequency f_ξ (diamond) from **a.** together with the calculated prediction $2f_p$ (grey shade) with $N \in [2, 5] \cdot 10^3$. **c.** Dependence of f_ξ (diamond) on total atom number N in coupled DW, $\mathcal{A} = 0.5$, and for comparison experimentally measured plasma frequency $2f_p$ (circle) and solid line marks the inferred $2f_p$ from Eq. 2.

On account of the observed squeezing oscillation in coupled DW, we develop an approach for preparing strongly correlated BECs in a decoupled DW. This is

of particular interest for their application as sensitivity-enhanced matter-wave interferometer[1, 2, 32]. We refer to this approach as two-step splitting (see Fig. 2b). The key of the two-step splitting is to optimise number squeezing with hold time in the coupled DW before exerting a second linear ramp to the decoupled DW at.

We show in Fig. 2c that the squeezing oscillation in the coupled DW is successfully preserved after transferring to the decoupled DW with two-step splitting and number squeezing is further enhanced during the second ramp. With this approach we obtain a phase coherence factor of $\langle \cos \Phi \rangle = 0.86^{+0.01}_{-0.02}$. This leads to a spin squeezing factor[5] of $\xi_s^2 = -9.2^{+1.9}_{-3.0}$ dB (with no detection noise correction, $\xi_s^2 = -4.0 \pm 1.1$ dB, see Methods), which witnesses many-body entanglement[28].

In contrast, single linear ramps yield lower spin squeezing factors of $\xi_s^2 \approx -1.5$ dB which demonstrates a significant gain with two-step splitting. A simple way to understand this is that two-step splitting enables us to achieve optimal number squeezing at an earlier stage of the splitting procedure and as a result, suppressing the phase diffusion more efficiently. This then grants an overall improved uncertainty in the phase space in the decoupled DW.

TUNING SQUEEZING OSCILLATIONS

To achieve controlled preparation of strongly correlated states with two-step splitting, it is crucial to understand the control parameters and tunability of the squeezing oscillation frequency. We identify two strategies: the first one involves tuning the parameters in a static BJJ, and the second one involves introducing time dependence on the control parameters through transversal excitation.

First, we explore experimentally the frequency scaling in elongated BJJ based on Eq.2. In Fig. 3a, we show the measured number squeezing oscillations in different DWs with decreasing single particle tunnel coupling J (bottom to top). We observe frequencies spanning more than one order of magnitude. In Fig. 3b, we plot collectively the extracted frequencies and as comparison the expectation of $2f_p$ (grey region) estimated directly from Eq.(2). Here, J for each \mathcal{A} is inferred from simulated DW potential and experimental atom number spanning $N \in [2, 5] \cdot 10^3$. We find good agreement between the experimental 1D BJJ and two-mode BH model. This confirms first of all that the observed squeezing oscillations indeed originate from stationary nonlinear Josephson dynamics.

The other DoF for tuning squeezing oscillation is the total atom number N . We fix DW configuration at $\mathcal{A} = 0.5$ and monitor the squeezing oscillations with varying N . In Fig. 3c we show experimentally measured squeezing oscillation frequency f_ξ as a function of N and compare them directly with experimentally measured plasma frequency $2f_p$ and a solid line derived from Eq.(2). In this strongly coupled DW, we can tune squeez-

ing oscillation frequency from 300 Hz to 800 Hz with only atom number.

To expand the tuning capabilities, we incorporate an active modulation on the tunnelling mechanism. By performing a splitting quench, we excite out-of-phase transverse sloshing between the two BECs at the transverse trap frequency $f_x = 1418(10)$ Hz. We depict in Fig. 4a this induced transversal motion with the inferred inter-condensate distance d after splitting at speed $\kappa = 0.085 \text{ ms}^{-1}$ to DW at $\mathcal{A} = 0.5$. This motional excitation drives the effective J periodically at the trap frequency f_x . We show in Fig. 4b how this periodic drive enforces ξ_N^2 to oscillate at comparable frequency with f_x . Furthermore, we can reproduce this oscillation frequency, with a two-step splitting quench to the decoupled DW (see Fig. 4c).

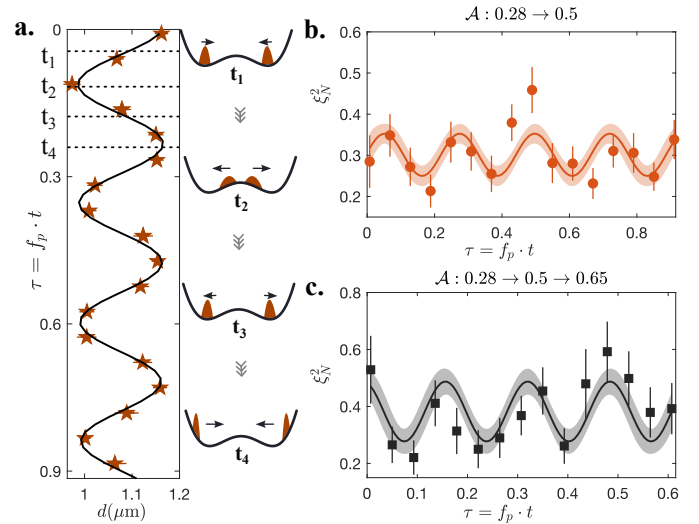


FIG. 4. **Driving number squeezing oscillation.** **a.** Inter-condensate distance d in 0.5 trap resulting from splitting quench with $\kappa = 0.085 \text{ ms}^{-1}$ into $\mathcal{A} = 0.5$ trap. d oscillates at the transverse trap frequency f_x . With this effective periodic modulation of tunnel coupling, we observe in **b.** that ξ_N^2 (orange circle) is driven at the trap frequency $f_x > f_p$. **c.** Transferred squeezing oscillation after two-step quench. τ indicates hold time in coupled DW.

By utilizing this method, we boost the preparation of spin-squeezed states with two-step in two ways: reduced ramp times as well as faster dynamics during the hold time. Our observations potentially facilitate investigations into captivating phenomena like parametric resonance[33] and Floquet engineering [34].

SQUEEZING-PROTECTED SPATIAL CORRELATIONS

With the gained insight on how to optimise spin squeezing, we now investigate how the spin squeezing influences the spatial correlations in our multimode sys-

tem. In a decoupled DW, number squeezing should prolong the global phase coherence and lead to reduced relative phase diffusion [32]. Indeed, we find a good qualitative agreement between experimentally extracted global phase diffusion rates and the global number squeezing (see Ext. Data Fig. 3).

The spatial resolution of our imaging system grants direct access to the local relative phase (see Methods). This allows us to explore how the observed number squeezing impacts the local dephasing[35, 36]. To study this,

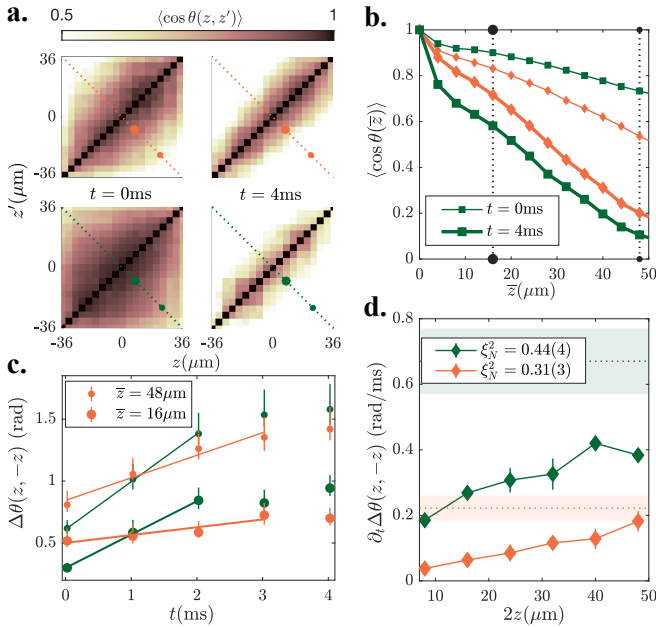


FIG. 5. Influence of number squeezing on multimode phase correlation function. **a.** Phase correlation function (PCF) $\langle \cos \theta(z, z') \rangle$ between two spatial positions z and z' along the condensates. Upper and lower panels show PCF of a state with $\xi_N^2 = 0.44(4)$ (orange) and $0.31(3)$ (green) at time t after splitting to DW at $\mathcal{A} = 0.6$. **b.** Spatially averaged PCF, $\langle \cos \theta(\bar{z}) \rangle$, with $\bar{z} = |z - z'|$ from **a.** visualises how number squeezing suppresses decay of PCF. **c.** Evolution of $\Delta\theta(z, -z)$ for $z = 8\mu\text{m}$ (big circle) and $z = 24\mu\text{m}$ (small circle). We infer the dephasing rate $\partial_t \Delta\theta(z, -z)$ with a linear fit and plot the extracted rates in **d** (see Ext. Data Fig. 4 for all distances z). The shaded regions represent extracted global phase diffusion rate. We observe a spatial dependence of $\partial_t \Delta\theta(z, -z)$ along the condensates, which hints on local number squeezing originating from the multimode dynamics of quasicondensates.

we prepare split BECs in an effectively decoupled DW ($\mathcal{A} = 0.6$), with two different levels of (global) number squeezing. We consider the relative phase field, $\theta(z, z') = \phi(z) - \phi(z')$, and the two-point relative phase correlation function (PCF), defined as $\langle \cos \theta(z, z') \rangle$.

In Fig. 5a, we compare the two-point PCF in the decoupled DW at two time instances, $t = 0$ ms and $t = 4$ ms, after initial preparation with $\xi_N^2 = 0.31(3)$ (upper panels) and $0.44(4)$ (lower panels). Despite higher PCF in the beginning, the decay is faster with weaker number squeezing

ing (lower panels). For better visualisation, we plot in Fig. 5b the averaged PCF, $\langle \cos \theta(\bar{z}) \rangle$, where $\bar{z} = |z - z'|$, in the central region $z = [-36, 36] \mu\text{m}$. It is evident that enhanced global number squeezing slows down the decay of PCF over large spatial separations \bar{z} .

For prethermalised states [37], it was found that the local number squeezing is directly linked to the effective temperature T^- according to the relation $T^- \propto \rho \xi_\rho^2$ (see [38] and App.). In multimode systems, different spatial modes can in principle feature different levels of squeezing; this would result in mode-dependent effective temperatures as for example in a generalized Gibbs ensemble [10]. To examine the spatial dependence of squeezing in our experiment, we track the time evolution of the fluctuations $\Delta\theta(z, -z)$ of the relative phase field between two symmetric points. We extract linear rates $\partial_t \Delta\theta(z, -z)$ and show an exemplary at two distances $z = 8\mu\text{m}$ and $24\mu\text{m}$ in Fig. 5c. We observe a spatial dependence of dephasing rates $\partial_t \Delta\theta(z, -z)$ (see Fig. 5d). As expected, experimental set with better global number squeezing yields an overall lower dephasing rate $\partial_t \Delta\theta(z, -z)$ and additionally we observe slower dephasing at small distances.

CONCLUSION AND OUTLOOK

We have observed oscillatory dynamics of quantum fluctuations on conjugate variables of a multimode BJJ and based on this observation, developed a more efficient approach for achieving better spin-squeezed states. We envision a more efficient preparation of spin-squeezed states with the help of optimal control algorithms optimizing the classical external dynamics after rapid two-step sequences. In consideration of our 1D multimode system, we have demonstrated the influence of number squeezing on prohibiting local dephasing in decoupled DWs. In future, the ability to track the squeezing dynamics provides a new way for optimizing the preparation of strongly correlated Sine-Gordon field simulators with lower effective temperatures; by experimentally approaching a regime which is dominated by quantum fluctuations, measurements of the entanglement entropy in quantum fields will become possible [39].

Acknowledgements

We thank Sebastian Erne, Camille Lévéque, and Igor Mazets for discussions and Philipp Kunkel for comments on the manuscript. This work is supported by the DFG/FWF CRC 1225 'ISOQUANT', (Austrian Science Fund (FWF) P 36236) and the QUANTERA project MENTA (FWF: I-6006). M.P. has received funding from the European Union's Horizon 2020 research and innovation program under the Marie Skłodowska-Curie grant agreement No 101032523.

Author contributions. T.Z. and M.P. took the experimental data with the help of Y.K., M.M. and F.B. T.Z. analysed the data with help of M.P. T.Z., Y.K., J.S. and M.P. discussed the experimental findings and wrote the

manuscript with the input from all authors. J.S. and M.P. supervised the work.

Author information

Correspondence and requests should be addressed to T.Z. (tiantian.zhang@tuwien.ac.at) or M.P. (maximilian.pruefer@tuwien.ac.at).

Data availability

Source data and all other data that support the plots within this paper and other findings of this study are available from the corresponding author upon reasonable request.

Competing financial interests

The authors declare no competing financial interests.

[1] Pezzè, L., Smerzi, A., Oberthaler, M. K., Schmied, R. & Treutlein, P. Quantum metrology with nonclassical states of atomic ensembles. *Rev. Mod. Phys.* **90**, 035005 (2018).

[2] Giovannetti, V., Lloyd, S. & Maccone, L. Quantum-enhanced measurements: beating the standard quantum limit. *Science* **306**, 1330–1336 (2004).

[3] Bloch, I., Dalibard, J. & Nascimbene, S. Quantum simulations with ultracold quantum gases. *Nature Physics* **8**, 267–276 (2012).

[4] Gühne, O. & Tóth, G. Entanglement detection. *Physics Reports* **474**, 1–75 (2009).

[5] Gross, C., Zibold, T., Nicklas, E., Esteve, J. & Oberthaler, M. K. Nonlinear atom interferometer surpasses classical precision limit. *Nature* **464**, 1165–1169 (2010).

[6] Riedel, M. F. *et al.* Atom-chip-based generation of entanglement for quantum metrology. *Nature* **464**, 1170–1173 (2010).

[7] Lücke, B. *et al.* Twin matter waves for interferometry beyond the classical limit. *Science* **334**, 773–776 (2011).

[8] Hamley, C. D., Gerving, C., Hoang, T., Bookjans, E. & Chapman, M. S. Spin-nematic squeezed vacuum in a quantum gas. *Nature Physics* **8**, 305–308 (2012).

[9] Esteve, J., Gross, C., Weller, A., Giovanazzi, S. & Oberthaler, M. K. Squeezing and entanglement in a Bose–Einstein condensate. *Nature* **455**, 1216–1219 (2008).

[10] Langen, T. *et al.* Experimental observation of a generalized Gibbs ensemble. *Science* **348**, 207–211 (2015).

[11] Schweigler, T. *et al.* Experimental characterization of a quantum many-body system via higher-order correlations. *Nature* **545**, 323–326 (2017).

[12] Gritsev, V., Polkovnikov, A. & Demler, E. Linear response theory for a pair of coupled one-dimensional condensates of interacting atoms. *Physical Review B* **75**, 174511 (2007).

[13] Coleman, S. Quantum sine-Gordon equation as the massive Thirring model. *Physical Review D* **11**, 2088 (1975).

[14] Smerzi, A., Fantoni, S., Giovanazzi, S. & Shenoy, S. Quantum coherent atomic tunneling between two trapped Bose–Einstein condensates. *Physical Review Letters* **79**, 4950 (1997).

[15] Raghavan, S., Smerzi, A., Fantoni, S. & Shenoy, S. Coherent oscillations between two weakly coupled Bose–Einstein condensates: Josephson effects, π oscillations, and macroscopic quantum self-trapping. *Physical Review A* **59**, 620 (1999).

[16] Albiez, M. *et al.* Direct observation of tunneling and nonlinear self-trapping in a single bosonic Josephson junction. *Physical review letters* **95**, 010402 (2005).

[17] Gati, R. & Oberthaler, M. K. A bosonic Josephson junction. *Journal of Physics B: Atomic, Molecular and Optical Physics* **40**, R61 (2007).

[18] Levy, S., Lahoud, E., Shomroni, I. & Steinhauer, J. The ac and dc Josephson effects in a Bose–Einstein condensate. *Nature* **449**, 579–583 (2007).

[19] LeBlanc, L. J. *et al.* Dynamics of a tunable superfluid junction. *Physical Review Letters* **106**, 025302 (2011).

[20] Spagnoli, G. *et al.* Crossing Over from Attractive to Repulsive Interactions in a Tunneling Bosonic Josephson Junction. *Phys. Rev. Lett.* **118**, 230403 (2017).

[21] Pigneur, M. *et al.* Relaxation to a phase-locked equilibrium state in a one-dimensional bosonic Josephson junction. *Physical review letters* **120**, 173601 (2018).

[22] Reichel, J. & Vuletic, V. *Atom chips* (John Wiley & Sons, 2011).

[23] Hofferberth, S., Lesanovsky, I., Fischer, B., Verdu, J. & Schmiedmayer, J. Radiofrequency-dressed-state potentials for neutral atoms. *Nature Physics* **2**, 710–716 (2006).

[24] Bücker, R. *et al.* Single-particle-sensitive imaging of freely propagating ultracold atoms. *New Journal of Physics* **11**, 103039 (2009).

[25] Castin, Y. & Dalibard, J. Relative phase of two Bose–Einstein condensates. *Phys. Rev. A* **55**, 4330–4337 (1997).

[26] Paraoanu, G.-S., Kohler, S., Sols, F. & Leggett, A. The Josephson plasmon as a Bogoliubov quasiparticle. *Journal of Physics B: Atomic, Molecular and Optical Physics* **34**, 4689 (2001).

[27] Wineland, D. J., Bollinger, J. J., Itano, W. M. & Heinzen, D. Squeezed atomic states and projection noise in spectroscopy. *Physical Review A* **50**, 67 (1994).

[28] Sørensen, A., Duan, L.-M., Cirac, J. I. & Zoller, P. Many-particle entanglement with Bose–Einstein condensates. *Nature* **409**, 63–66 (2001).

[29] Milburn, G., Corney, J., Wright, E. M. & Walls, D. Quantum dynamics of an atomic Bose–Einstein condensate in a double-well potential. *Physical Review A* **55**, 4318 (1997).

[30] Xin, L., Chapman, M. & Kennedy, T. Fast Generation of Time-Stationary Spin-1 Squeezed States by Nonadiabatic Control. *PRX Quantum* **3**, 010328 (2022).

[31] Xin, L., Barrios, M., Cohen, J. T. & Chapman, M. S. Squeezed Ground States in a Spin-1 Bose–Einstein Condensate (2022). URL <https://arxiv.org/abs/2202.12338>.

[32] Berrada, T. *et al.* Integrated Mach–Zehnder interferometer for Bose–Einstein condensates **4**, 2077.

[33] Lovas, I. *et al.* Many-body parametric resonances in the driven sine-Gordon model. *Phys. Rev. B* **106**, 075426 (2022).

[34] Ji, S.-C. *et al.* Floquet engineering a bosonic Josephson

junction. *Physical Review Letters* **129**, 080402 (2022).

[35] Kitagawa, T., Imambekov, A., Schmiedmayer, J. & Demler, E. The dynamics and prethermalization of one-dimensional quantum systems probed through the full distributions of quantum noise. *New Journal of Physics* **13**, 073018 (2011).

[36] Bistritzer, R. & Altman, E. Intrinsic dephasing in one-dimensional ultracold atom interferometers. *Proceedings of the National Academy of Sciences* **104**, 9955–9959 (2007).

[37] Gring, M. *et al.* Relaxation and Prethermalization in an Isolated Quantum System. *Science* **337**, 1318–1322 (2012).

[38] Erne, S. A. *Far-From-Equilibrium Quantum Many-Body Systems: From Universal Dynamics to Statistical Mechanics*. Ph.D. thesis (2018). URL <http://www.ub.uni-heidelberg.de/archiv/25106>.

[39] Tajik, M. *et al.* Experimental verification of the area law of mutual information in quantum field theory (2022). URL <https://arxiv.org/abs/2206.10563>.

[40] Javanainen, J. & Wilkens, M. Phase and phase diffusion of a split Bose-Einstein condensate. *Physical Review Letters* **78**, 4675 (1997).

[41] Leggett, A. & Sols, F. Comment on “Phase and Phase Diffusion of a Split Bose-Einstein Condensate”. *Physical review letters* **81**, 1344 (1998).

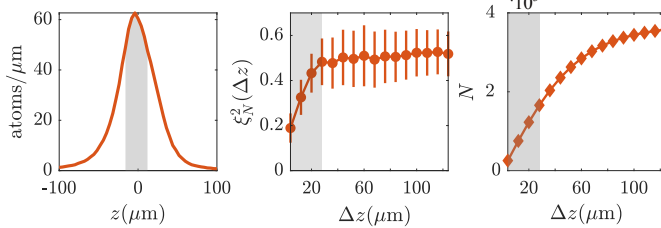
METHODS

Number squeezing factor estimation

We sum the signal from both cloud to obtain the global number of counts S_L and S_R and calculate the global number squeezing factor by

$$\xi_N^2 = \frac{\Delta^2 S_- - 2S - 2\Delta^2 b}{\bar{p}S}. \quad (4)$$

Here $\Delta^2 S_- = \Delta^2(S_L - S_R)$ is the variance on the relative photon signal, \bar{p} is the experimentally calibrated average number of photons collected per atom and $\Delta^2 b$ is the variance of background noise of an atom-free-region on the EMCCD chip. Noise of $2S = 2(S_L + S_R)$ originates from the electron multiplication process of the EMCCD chip. $2S + \Delta^2 b$ is the combined detection noise which is indicated as grey dotted line (Gaussian with corresponding width) in the histogram of N_- in Fig. 1d.



Ext. Data Fig. 1. Imaging influence on spatially resolved number squeezing detection. Left panel: Longitudinal profile of BEC. Middle panel: Influence of finite integration length Δz on evaluation of number squeezing factor ξ_N^2 . Δz is evaluated symmetrically around the peak density along the condensate. Right panel: Atom number N within integration region Δz . Shaded region indicates the lower bound of Δz for reliable estimation of ξ_N^2 .

The longitudinal extension of the condensates is $L = 60 - 120 \mu\text{m}$ depending on the total atom number. Due to random walk of atoms in the imaging light and diffusion of emitted photons, the effective imaging resolution is larger than pixel size δz , where $\delta z = 4 \mu\text{m}$ denotes the optical imaging resolution. The effective imaging resolution is critical for evaluation of local number squeezing factor. We show in Ext. Data Fig. 1 that the calculated ξ_N^2 reaches a steady value with integration regions above $\Delta z = 28 \mu\text{m}$. This length signifies the effective resolution which is still a few times smaller than the condensate length.

Extraction of relative phase

We fit the interference fringe slice-wise with $\rho(x) \approx g(x)[1 + C \cos(k_0(x - x_0) + \phi)]$ to extract the local relative phase ϕ and the fringe visibility C , indicating the single

particle coherence. To minimize the readout error originating from the locally fluctuating relative phases, we extract the global relative phase $\Phi = \arg(\exp(i\phi(z)))$, based on independently fitted local relative phase $\phi(z)$ over region $z = [-3, 3]\delta z$.

Fit and errorbars

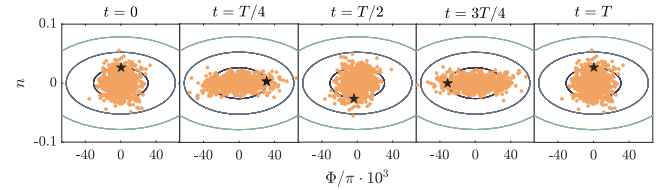
Squeezing oscillations are fitted with function $\xi(t) = a \cdot \sin(2\pi f_\xi \cdot t + p_0) + \bar{\xi}$ with a, f_ξ, p_0 and $\bar{\xi}$ as its fit parameters. Shaded region of fitted model signifies 68% simultaneous bound prediction confidence intervals of fit function. Errorbars on experimentally measured squeezing factors values are estimated standard error using jackknife.

Semi-classical simulation on squeezing oscillations

To visualize the squeezing oscillation in the coupled DW (see Fig. 2), we set up a semi-classical simulation. In Ext. Data. Fig. 2, we plot the equipotential lines in the classical phase space given by the two-mode Bose-Hubbard model

$$\mathcal{H} = \frac{2J}{\hbar} \left[\frac{UN}{4J} n^2 - \sqrt{1 - n^2} \cos \Phi \right], \quad (5)$$

with suitable parameter values for DW $\mathcal{A} = 0.5$: single particle tunnel coupling energy $J = 41.5 \text{ Hz}$, interaction energy $U = 0.33 \text{ Hz}$ and total atom number $N = 3500$. Here J is estimated using the energy difference between the two lowest single particle eigenstates in the simulated DW potential, $J = (E_1 - E_0)/2$, and experimentally measured atom number N .



Ext. Data Fig. 2. Propagation of imprinted initial fluctuations in the two-mode BH model. The star marker signifies the evolution of a single realisation, representing the mean field value. A π rotation of a single realisation corresponds to a 2π rotation of the phase space fluctuations. Here T is one period of Josephson oscillation.

Around the stable fixed point and given small fluctuations in the lower energy states, BH Hamiltonian can be further linearized and expressed in harmonic approximation as

$$H_{hc} = \frac{hf_p}{2} \left(\frac{\Phi^2}{2\Delta_{SG}^2 \Phi} + \frac{N_-^2}{2\Delta_{SG}^2 N_-} \right), \quad (6)$$

where $\Delta_{SG}^2 \Phi = \sqrt{1 + \Lambda}/N$ and $\Delta_{SG}^2 N_- = N_-/\sqrt{1 + \Lambda}$ are ground state fluctuations. With these parameters, we can estimate the expected ground state squeezing factors in Eq. 6 to be $\xi_N = 1/\sqrt{1 + \Lambda}$ and $\xi_\phi = \sqrt{1 + \Lambda}$.

We sample 1000 realisations from two normal distributions (one for each observable) with variances larger than the ground state fluctuations Δ_{SG}^2 (deduced from Eq. 6) and propagate them with equations of motion deduced from Eq. 5 in the classical limit. We show in Ext. Data Fig. 2 the simulation result of quantum state propagation in a time span of $T = 1/f_p$, where T corresponds to a period of Josephson oscillation of the expectation value of the observables (star marker). As one can see, the projection noise in each observable oscillates at twice the frequency as the expectation values, namely $f_\xi = 2f_p$.

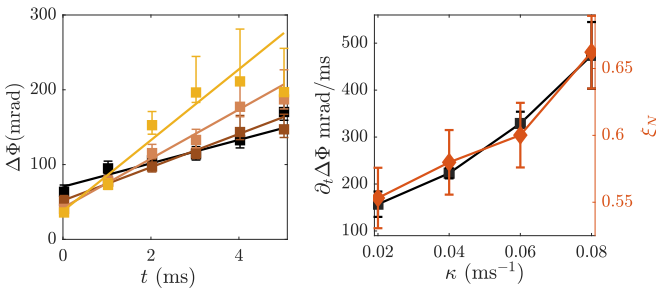
Impact of number squeezing on global phase diffusion

In decoupled trap ($J \approx 0$), phase diffusion after symmetric splitting[40, 41] can be expressed as

$$\Delta^2 \Phi(t) = \Delta^2 \Phi_0 + R^2 t^2, \quad (7)$$

where $R = \frac{\xi_N \sqrt{N}}{\hbar} \frac{\partial \mu}{\partial N} \Big|_{N=N/2}$ is the phase diffusion rate and $\Delta^2 \Phi_0$ is the initial variance of Φ right after splitting and $\mu(N)$ is the chemical potential of BEC with atom number N . Eq. 7 implies slower phase diffusion with stronger number squeezing.

We investigate experimentally the influence of number squeezing on global phase diffusion rate by splitting into effectively decoupled DW, $\mathcal{A} = 0.6$. For different split speed κ we measure the phase spread $\Delta\Phi(t)$ and deduce the phase diffusion rate from a linear fit. The extracted rates $\partial_t \Delta\Phi$ match the trend of the measured ξ_N . (see Ext. Data. Fig. 3).



Ext. Data Fig. 3. Global number squeezing suppresses global phase diffusion in decoupled trap. Left panel: phase diffusion in $\mathcal{A} = 0.6$ trap for different splitting speeds κ . Right panel: The linearly fitted phase diffusion rates $\partial_t \Delta\Phi$ agree qualitatively with the measured ξ_N with different κ .

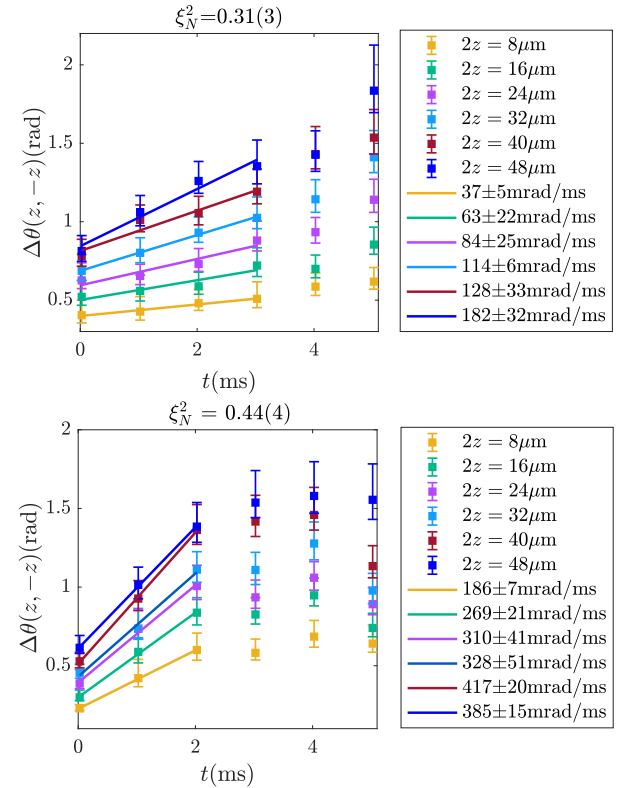
Impact of number squeezing on spatial dephasing

For resolving local dynamics between two split 1D condensates, we introduce the local observables along the condensates: the local relative phase $\phi(z) = \phi_L(z) - \phi_R(z)$ and the relative density $\rho_-(z) = \rho_L(z) - \rho_R(z)$. The local and global observables fulfill the relation $\Phi = \arg(\exp(i\phi(z)))$, $N_- = \sum_z \rho_-(z)$.

In previous works studying the phenomenon of prethermalisation [35, 37], the effective temperature T^- between the two condensates was connected to the relative density fluctuations $\Delta^2 \rho_- = \langle \rho_-^2 \rangle$ by

$$T^- = \frac{g \Delta^2 \rho_-}{2} = \frac{g \rho_0 \xi_\rho^2}{2}, \quad (8)$$

where ρ_0 is the peak atomic density in each condensate after splitting and ξ_ρ^2 is the local number squeezing factor.



Ext. Data Fig. 4. Extraction of local dephasing rates in decoupled trap in relation to global number squeezing. Evolution of spatial relative phase fluctuations $\Delta\theta(z, -z)$ between two symmetrically located points around the longitudinal center of the BEC. Upper panel: $\Delta\theta(z, -z)$ evolution with global number squeezing $\xi_N^2 = 0.31(3)$ and a linear fit on the four first time instances. Lower panel: $\Delta\theta(z, -z)$ evolution with global number squeezing $\xi_N^2 = 0.44(4)$ and a linear fit on the three first time instances.